Cooling of Rydberg H̄ during radiative cascade

C L Taylor, Jingjing Zhang and F Robicheaux

Department of Physics, Auburn University, AL 36849-5311, USA

Abstract
We have simulated the centre-of-mass motion of Rydberg anti-hydrogen atoms in spatially varying magnetic fields. We find that a population of anti-hydrogen can lose substantial centre-of-mass kinetic energy during the radiative cascade to the ground state. The loss of energy is due to the change in magnetic moment when photons are emitted and is akin to adiabatic cooling. We also simulate the pattern of anti-hydrogen hits on the walls of the trap and find that the existence of trapped Rydberg atoms leads to a distinctive distribution along the trap axis.

1. Introduction

Recently, two groups [1, 2] reported the formation of anti-Hydrogen (H̄) by having anti-protons (p̄) traverse a positron (e⁺) plasma. Presumably [3–5], the H̄ is formed through three body recombination (TBR): two e⁺'s scatter in the field of the p̄ so that one e⁺ loses enough energy to become bound to the p̄ and the other e⁺ carries away the excess energy. This gives highly excited (Rydberg) H̄. Double charge transfer [6–8] has also been used [7] to make Rydberg H̄ although the number of produced H̄'s seems to be greatly reduced from those formed through TBR.

The next goal of H̄ experiments is to trap the atoms for spectroscopic measurements. The trapping will be attempted through the use of spatially varying magnetic fields with the magnetic field having a minimum where H̄ is formed. As in many other neutral atom traps, the handle on the atoms is their magnetic moment with only the population attracted to low fields getting trapped. This trapping will be hampered by the fact that the current versions of the experiments make atoms with centre-of-mass kinetic energies substantially higher than the temperature of the e⁺ plasma [9–11]. The double charge transfer presumably makes H̄ with centre-of-mass kinetic energy comparable to that of the p̄ plasma but the production rate is low compared to TBR [7] and the atoms formed in strong B-fields are preferentially attracted to fields [8] which will reduce the trappable population. For this paper, we assume that the problem of hot H̄ has been solved and the next generation H̄ experiments will give centre-of-mass temperatures within a factor of ~ 10 of the e⁺ or p̄ plasmas. To increase the magnetic trap depth, these experiments will be performed in magnetic fields substantially smaller than in the original experiments: 1–2 T compared to 4–5.5 T.

We make two predictions about the effect of spatially varying magnetic fields on Rydberg H̄. (1) The radiative cascade of Rydberg H̄ will lead to a population of H̄ whose centre-of-mass temperature cools as the magnetic moment decreases. This will be a mechanism to give more trapped H̄ than might be expected and their temperatures will be lower. (2) The pattern of annihilation on the walls of the trap will also contain a population with a larger than expected spatial spread. While simple arguments are sufficient to convince one that these predictions must be correct, the size of the effect can only be determined by a more detailed treatment. The centre-of-mass energy is defined to be the kinetic energy of the atom plus the energy shift of the Rydberg state measured from the centre of the trap: $E_{\text{com}} \simeq KE + [B(\vec{r}) - B(0)]\mu_{\text{B}}m$, where μ_{B} is the Bohr magneton and m is the azimuthal quantum number.

In this paper, we present a detailed treatment of how radiative cascade of Rydberg states affects the centre-of-mass temperature of H̄ and the spatial pattern of annihilations. One can intuitively see that there will be an effect by imagining how the centre-of-mass potential of the H̄ behaves during the cascade. The magnetic fields will be generated so that the minimum in $B \equiv |\vec{B}|$ is in the region where H̄ is formed. B increases as H̄ travels toward the wall of the trap *and* as it travels along the trap away from the region of formation. In many circumstances [8, 12], the majority of H̄ will be attracted to high fields and these will be quickly expelled from the trap. This effect leads to a decrease in the population of trappable H̄ from simple estimates. There does not appear to be any practical method for converting atoms attracted to high fields into those attracted to low fields before they annihilate. Therefore, we ignore the population attracted to high fields throughout this paper.

However, a fraction of the population will be attracted to low fields and these can have a large enough magnetic moment to be trapped. Because these are highly excited states, they can have magnetic moments substantially larger than a Bohr magneton. As the atoms radiatively cascade to lower levels, the magnitude of the magnetic moment will also tend to decrease. Since the centre-of-mass potential of H̄ is proportional to the magnetic moment times the magnetic field, the potential will appear to be 'opening up' and decreasing with time. This is equivalent to keeping the magnetic moment fixed but decreasing the strength of the magnetic field. Thus, there will be adiabatic or diabatic cooling depending on the decay rate.

This qualitative description lead us to suspect that the ground state atoms will have less centre-of-mass energy than the original Rydberg H̄. Thus, we expect that the fraction of trapped H̄ in the ground state will be larger than a simple estimate using the centre-of-mass energy of the Rydberg H̄. The purpose of this paper is to draw attention to this mechanism and to investigate the dependence of the final temperature on properties of the initial state and the magnetic field. This cooling effect has been noted in [13] and [14].

The temporary trapping of Rydberg H̄ also affects the pattern of annihilations on the walls of the trap. Because the Rydberg H̄ travels substantial distances between photon emissions, the pattern of annihilations on the walls of the trap will extend further from the region where H̄ are created. Thus, a measurement that shows a spatially broad distribution of annihilations on the wall of the trap can be taken as a sign of trapped Rydberg H̄.

For this paper, we only consider the cascade with states $n \leqslant 25$. The reason for this restriction is that the main effects occur for $n \leqslant 15$. In previous experiments, the atoms are mostly made with higher principal quantum number and large ℓ so that we are assuming these states survive in the trap to cascade to the lower n's that we treat. The vast majority of atoms that can be trapped will pass through the states that we treat here.

All of the results of this paper could be tested using ordinary matter, hydrogen. The physics is due to the correlation between the time-dependent decrease of the magnetic moment and the strength of the magnetic field.

2. Basic theory

In this section, we describe the elements of our calculation and the reasons for our choices of computational techniques. All of the choices described in this section involve approximations which we have made to simplify the problem.

2.1. General approximations

The motion of H̄ through the traps is an intractable computational problem for the time scales of the radiative cascade. Typical time scale for the cascade is roughly ms for states near $n = 25 - 30$. However, the internal time scale of the atom is roughly ps which is a billion times shorter. We are forced to make several approximations so the calculations can be completed in reasonable time. This section describes the general approximations. The later subsections describe the more detailed approximations.

The H̄ traps have macroscopic sizes and the variations of the fields in the traps are also over macroscopic distances (roughly cm). Therefore, we do not need to treat the centre-of-mass motion of H̄ at the quantum level: the de Broglie wavelength of H̄ is more than a factor of 10^7 smaller than the size scale of the trap. However, the photon emission is a quantum process so we treat the internal degrees of freedom of the atom using quantum mechanics.

The magnetic field perturbs the zero field states through the diamagnetic interaction potential. However, this perturbation is small. For example, the diamagnetic energy shift divided by the Rydberg spacing is ~ 0.015 for $n = 25$ in a 1 T field.

The centre-of-mass coordinates are not separable from the internal coordinates in an external magnetic field. When the period of the internal motion is short or the magnetic field weak, the motions nearly separate. At this level, the strongest effect is the motional Stark effect which gives an apparent electric field for the internal motion with a magnitude $|\vec{E}| = |\vec{v} \times \vec{B}|$ where we have used SI units. To see the size of this effect, we use the thermal velocity $v = \sqrt{2k_B T / M_{\bar{H}}} \simeq 260$ m s^{-1} at 4 K. This translates to E $\simeq 260$ V m^{-1} = 2.6 V cm^{-1} for $B = 1$ T. Taking the dipole moment to be $ea_0 n^2$, where e is the electric charge, a_0 is the Bohr radius and n is the principal quantum number which gives an energy shift of ~ 0.1 K for an $n = 30$ state. The energy shift due to the magnetic moment is $eB\hbar m/(2M_e) = 0.67$ m B K/T, where M_e is the electron mass and m is the azimuthal quantum number. Taking $m = n/2$ gives an energy shift of $\simeq 10$ K. We feel it is a good approximation to ignore the motional Stark effect.

The H̄ traps also contain electric fields to hold the e$^+$ plasma and p̄'s within a given region. These fields can be as large as ~ 30 V cm^{-1} which is roughly a factor of 10 larger than the motional Stark field. The energy shifts from the applied electric fields are still approximately a factor of 10 less than that from the magnetic field. We feel that the external electric fields can also be neglected especially since we assumed the atom has an electric dipole moment comparable to its largest possible value whereas the electric dipole moment in a strong magnetic field is substantially reduced.

The internal states of the atom are subject to time-dependent electric and magnetic fields due to the motion of H̄ through the spatially varying fields. In principle, this can cause transitions between the Rydberg states of the atom. We have neglected this effect and have assumed that the internal state of the atom adiabatically follows the fields. This seems to be a good approximation because the time over which the fields varies is much longer than the periods of motion in the atom. The fields vary over a length scale of roughly a cm whereas the speed of the atom is a few 100 m s^{-1}. Thus, the time scale of the field variation is longer than 10 μs. However, the periods of internal motion of the atom is approximately ps for radial

motion and 10–100 ps for states within an n-manifold. Thus, there is at least a factor of 10^5 difference in the time scales.

We have not quantitatively accounted for the ℓ-mixing and energy shifts of the atomic states due to the diamagnetic term (proportional to $B^2 r^2 \sin^2 \theta$) in the Hamiltonian. Since we will be investigating states with $n < 40$ and magnetic fields less than 2 T, the eigenstates do not mix n. In the ℓ-mixing region the diamagnetic term always *increases* the energy of the state. Thus, this term will add to the trapping force. In a 1 T field, the $n = 30, m = 0$ states split into states with almost no energy shift to states with $\sim$1.4 K energy shift; but the $n = 30, m = 10$ states get a maximum shift from the diamagnetic potential of $\sim$1.0 K and the $m = 20$ states get a maximum shift of $\sim$0.6 K. We have neglected this shift because it is roughly an order of magnitude less than the shift from $\vec{L} \cdot \vec{B}$. The size of the shift scales with n^4 so it rapidly becomes completely negligible as n decreases. Perhaps more importantly, the ℓ-mixing will change the radiative cascade. For a given m, the diamagnetic potential mixes together states with $\ell = |m|, |m| + 2, |m| + 4, \ldots$ and mixes together states with $\ell = |m| + 1, |m| + 3, |m| + 5, \ldots$. The radiative cascade of ℓ-mixed states is extremely complicated. To avoid this complication, we either used states with $\ell = |m| = n - 1$ (for which there is no mixing) or used the approximation described in section 2.4.

In our calculations, the only mechanism for changing the state of the atom is photon emission. However, collisions can change the state of the atom every time H̄ goes through the e$^+$ cloud. The e$^+$–H̄ collisions can change n and can change the magnetic moment. Unfortunately, the size of the effect depends strongly on the density, size, and shape of the e$^+$ plasma. These are quantities that will depend on specific experimental details which are unavailable. For an e$^+$ plasma that is dense enough and large enough, e$^+$–H̄ collisions could dominate the state changing rates for $n \sim 25$ and higher. We performed classical scattering calculations to find how rapidly the magnetic moment changes. For $n = 25$ states, we found that the magnetic moment does not significantly change over 15 μs when immersed in a 4 K plasma with a density of 10^7 cm^{-3}; this time is somewhat over-restrictive since the character of the m distribution is mostly unchanged up to 30 μs. This is shorter than the lifetime of high-m $n = 25$ states but the atom does not spend all of its time inside the plasma. We will estimate the density of e$^+$ that will start affecting our calculations.

Lastly, the collision between fast p̄'s (few eV) and H̄ can cause ℓ, m changes. The fast p̄ are present due to the trapping electrodes. Fortunately, the magnetic field strongly suppresses these collisions; without the magnetic field, the atoms would suffer too many ℓ, m changing collisions to reach the ground state. We computed the rate for this process by solving the close coupling equations within an n-manifold and found that the rate is less than 2×10^{-2} cm^3 s^{-1} for $n = 25$ in a 1 T field with the p̄ energy of 5 eV. Since the photodecay rate for $n = 25$ is $\sim$1700 Hz, the ℓ, m changing probability will be less than 0.1 as long as the p̄ density is less than $\sim$10^4 cm^{-3}; the lower n decay faster and have smaller collision rates and, thus, will be less affected by collisions. The experiment reported in [1] was well below this density while [2] had a range of densities from below this cutoff to above it. It is likely that the next generation experiments will be below this density.

The size of the errors in our approximations increases rapidly with increasing n. H̄ experiments will produce atoms with a wide range of n. Our results are most applicable to atoms with $n < 30$.

2.2. Magnetic field configuration

The spatial dependence of the magnetic field must have several properties and is constrained by the physical geometry of the H̄ traps and the necessity for holding charged particles. The

traps are cylinders whose length is much larger than the radius. To facilitate this description and those further in this paper, we will take z to be the direction along the trap axis, ρ to be the distance out from the axis, and ϕ to be the angle around the axis. The origin will be taken to be the centre of the e^+ cloud where H̄ is formed.

We will generate the full magnetic field as a superposition of three types of fields: a uniform field along the trap axis, a field from two mirror coils that give fields that increase/decrease along the axis, and a field from wires parallel to the trap axis that make a multipole field that increases with ρ. The magnitude of the magnetic field is substantially less than that in the previous experiments [1, 2] due to the need for trapping H̄; the trap depth increases as the size of the uniform magnetic field decreases.

There must be a substantial magnetic field, B_0, along the z-direction to trap the charged particles. p̄'s and e^+ are confined in ρ by this magnetic field.

In order to trap H̄, the magnetic field needs to increase away from the origin. The motion along the trap axis can be restricted by adding two mirror coils at a distance $\pm L/2$. Each coil is actually a short solenoid whose length is much less than L with the coil axis parallel to the trap axis. The coils are arranged so the magnetic field at the centre is parallel to the uniform magnetic field. The magnetic field from the coil decreases as you move along the axis away from the coil. This means the sum of the magnetic field from the two coils, $\vec{B}_{mc}$ gives a magnetic field minimum at the origin.

The H̄ motion perpendicular to the trap axis is constrained by a multipole field from wires mainly parallel to the trap axis. For a large portion of the trap, the magnetic field from these wires can be approximated by a pure multipole field:

$$\vec{B}_{mp} = B_w \left(\frac{\rho}{\rho_w} \right)^{s-1} (\sin[(s-1)\phi], \cos[(s-1)\phi], 0), \tag{1}$$

where B_w is the magnitude of the field at the trap wall, ρ_w is the radius of the trap, and we have chosen the xy-directions so the field is in the y-direction at $\phi = 0$. Since this field is perpendicular to the uniform field, the multipole field strength at the wall of the trap will need to be comparable to that for the magnetic field along the trap axis. The change in B is $\Delta B = \sqrt{B_0^2 + B_w^2} - B_0$ determines the potential well depth for H̄; for a given B_w, the trap depth decreases as B_0 increases which is the motivation for making B_0 smaller than in the previous experiments. Remember that a change in magnetic field of 1 T gives a well depth of approximately 2/3 K for the ground state. Experimental studies [16] have shown that the multipole field strength at the wall needs to be weaker for lower order multipoles. Therefore, it seems likely that the H̄ traps will use higher multipole order.

2.3. Atom motion

The time-dependent motion of the atom was computed using an adaptive step size, fourth-order Runge–Kutta method. During a time step, the magnetic moment of the atom was assumed to be constant. This is equivalent to not allowing a photon emission during the Runge–Kutta step. The shift in internal energy of the atom was taken to be

$$U(\vec{r}) = \mu_B m B(\vec{r}), \tag{2}$$

where $\mu_B = e\hbar/2M_e$ is the Bohr magneton, m is the azimuthal quantum number and $B(\vec{r}) = |\vec{B}(\vec{r})|$ is the magnitude of the magnetic field. We define the centre-of-mass energy of H̄ to be its kinetic energy plus the energy shift of its internal state from the centre of the trap: $E = KE + U(\vec{r}) - U(0)$. The force on the centre of mass of the atom is

$$\vec{F}(\vec{r}) = -\vec{\nabla} U = -\mu_B m \vec{\nabla} B(\vec{r}). \tag{3}$$

Due to the complicated spatial dependence of B, we computed the divergence of B by a two point, central difference: $dG(x)/dx \simeq [G(x+\delta x) - G(x-\delta x)]/2\delta x$. We insured the stability and accuracy of our calculations by doing several runs with different values of $\delta x, \delta y, \delta z$ in the computation of $\vec{\nabla} B$; the error from this low-order approximation to the force was less than the error from the numerical time stepping (Runge–Kutta) part of the calculation. We also performed several calculations for different accuracy parameters in the adaptive step-size Runge–Kutta method. In typical trajectories, the energy was conserved to better than a part in 10^9.

In all of the calculations, we numerically followed the motion of the atoms until they hit the wall of the trap or reached the z-position of the mirror coils. Of course, the trapped atoms can not reach these positions. Therefore, we computed the atom's total energy once it reached the ground state and compared this with the minimum energy needed to reach the trap wall. If its energy is greater than the minimum needed to reach the wall, we continue the propagation until it hits. If the energy is less than the minimum needed to reach the wall, further propagation is not necessary.

2.4. Time dependence of atomic states

Our treatment of the time dependence of the atomic states involves approximating the radiative decay rates and approximating the energy shifts of the states with B. Our approximations were compared to fully quantum calculations [15]. Because we are using magnetic fields between 1–2 T and internal states with $n \leqslant 25$, these approximations are accurate to better than 20% with the largest inaccuracy for $n = 25$. As will be seen in the results section, the largest effect occurs for $n \leqslant 15$ where the approximations are accurate at the per cent level. Test runs with the fully quantum parameters rarely showed changes larger than a per cent; actually, the size of the effect is slightly increased with the full quantum calculation in strong B because the radiative decay rate is higher at larger B. We have used these approximations instead of the full quantum results because it will then be clear that the main effects result from simple physical processes and is not dependent on complicated quantum calculations.

The only process that causes the internal quantum state to change is the radiative cascade. We mainly investigated two cases: states with $\ell = |m| = n - 1$ and a semi-classical approximation to the cascade for a distribution of starting $|m|$. In both cases, we used a Monte Carlo method for deciding when the photon was emitted.

For most of the calculations, we started the atom in the 'circular' state with $\ell = |m| = n - 1$. We chose this starting state because radiative cascades from higher states tend toward $\ell \sim n$. Also, our approximations (especially ignoring electric fields and ℓ-mixing from external fields) hold best for this state. Therefore, we are guaranteed that our results are not artefacts of any approximation used in our simulations. For this case, the radiative cascade can only take the state to the state with n, ℓ, m each decreased by 1 which again gives a circular state. This was accomplished by a Monte Carlo procedure. We compared the probability for photon emission during the time step, $\Gamma_n \delta t$, to a single random number x with a flat distribution between 0 and 1. If $x < \Gamma_n \delta t$, then the photon is emitted and the quantum numbers all decrease by 1. For a typical step in the Runge–Kutta propagation, $\Gamma_n \delta t \ll 1$ which means there were many time steps between photon emissions. We evolve the state in time using the radiative decay rate of a circular state which to a very good approximation[1] is given by

---

[1] This formula is an approximation to the exact quantum $B = 0$ decay rate and is accurate to 5% for $n = 2$, 0.5% for $n = 5$, and becomes rapidly more accurate still as n increases. At high n, the radiative decay becomes larger than this in strong B because the energy separations increase. For a 1 T field, the actual quantum rate is larger by $\sim 2\%$ at $n = 15$ and $\sim 10\%$ at $n = 25$. For a 2 T field, the actual quantum rate is larger by $\sim 4\%$ at $n = 15$ and by $\sim 20\%$ at $n = 25$.

$$\Gamma_n = \frac{1.61 \times 10^{10} \text{ Hz}}{(n - 1/2)^2 n^3}. \tag{4}$$

Using a B independent decay rate underestimates the true decay rate for higher n for spatial regions where B is larger; thus, this approximation reduces the size of the effect seen in the results section.

We performed separate calculations for $|m| < \ell$. Due to the complex nature of the fields and cascades, these are much more approximate in nature. The purpose of these calculations was to check whether our results strongly changed if we removed the requirement of $n \to n - 1 \to n - 2$ etc in our cascade. It is known that a classical treatment [17] of the cascade gives the equations

$$\frac{\mathrm{d}n}{\mathrm{d}t} = 1.61 \times 10^{10} \text{ Hz} \frac{3n^2 - \ell^2}{3n^2 \ell^5} \tag{5}$$

$$\frac{\mathrm{d}\ell}{\mathrm{d}t} = 1.61 \times 10^{10} \text{ Hz} \frac{2}{3n^3 \ell^2}. \tag{6}$$

Note that the rate $\mathrm{d}n/\mathrm{d}t$ is greater than $\mathrm{d}\ell/\mathrm{d}t$. In particular, the n decay rate rapidly increases as ℓ decreases.

We use these in a Monte Carlo procedure to approximate a fully quantum cascade. After each Runge–Kutta step, the probabilities for change during δt, $\delta t \, \mathrm{d}n/\mathrm{d}t$ and $\delta t \, \mathrm{d}\ell/\mathrm{d}t$, were compared to a single random number, x_{ran}, with a flat distribution between 0 and 1. There were three possible outcomes: (1) if $x_{\mathrm{ran}} > \delta t \, \mathrm{d}n/\mathrm{d}t$ then neither n nor ℓ were changed, (2) if $\delta t \, \mathrm{d}\ell/\mathrm{d}t < x_{\mathrm{ran}} < \delta t \, \mathrm{d}n/\mathrm{d}t$ then $n \to n - 1$ but ℓ did not change and (3) if $x_{\mathrm{ran}} < \delta t \, \mathrm{d}\ell/\mathrm{d}t$ then $n \to n - 1$ and $\ell \to \ell - 1$. Case (1) is by far the most likely outcome. If $\ell \to \ell - 1$, then m can also change. Classically, m/ℓ does not change due to radiation of light. This means that if that atom starts with ℓ, m on average $m \to m - (m/\ell)$ when $\ell \to \ell - 1$. Therefore, when $\ell \to \ell - 1$, we get another random number and if it is less than m/ℓ then we also have $m \to m - 1$. This cascade goes over to the circular case when $|m| = \ell = n - 1$. The approximations in this cascade should be sufficiently accurate for our purposes.

Lastly, the magnetic field can mix ℓ if $|m| < \ell - 1$. This is an extremely difficult process to include with radiative cascade so we resorted to a heuristic treatment. To incorporate this effect, we use the ℓ-mixing period which is roughly $\tau_{\mathrm{mix}} \sim 15 \mu s/(B^2 n^3)$ (with B in T) to randomize ℓ between $|m|$ and $n - 1$. The ℓ-mixing period is taken from $h/\Delta E$, where h is Planck's constant and ΔE is the spacing between diamagnetic states within an n-manifold. After each Runge–Kutta step, we compare $\delta t/\tau_{\mathrm{mix}}$ to a random number between 0 and 1. If the random number is less than $\delta t/\tau_{\mathrm{mix}}$, we change ℓ to $|m| + (n - 1 - |m|)y_{\mathrm{ran}}$, where y_{ran} is another random number with a flat distribution between 0 and 1. This treatment allows for a range of ℓ for a given $|m|$. It also has ℓ change on roughly the correct time scale. While this is clearly not a quantum treatment of the diamagnetic ℓ-mixing, it does have many of the correct features and should give qualitatively correct results.

3. Trap configuration

It is clear that the sizes and details of the traps and the size of the three different fields is not known at this time. However, we can make choices based on previous experiments that are likely to be approximately correct.

For all of the calculations below, we used the following parameters. The uniform field along the axis was 1 T. The radius of the trap was 2.3 cm. The distance between the mirror coils was 24 cm. We approximated the coils by a single loop of wire with a radius of 3.6 cm
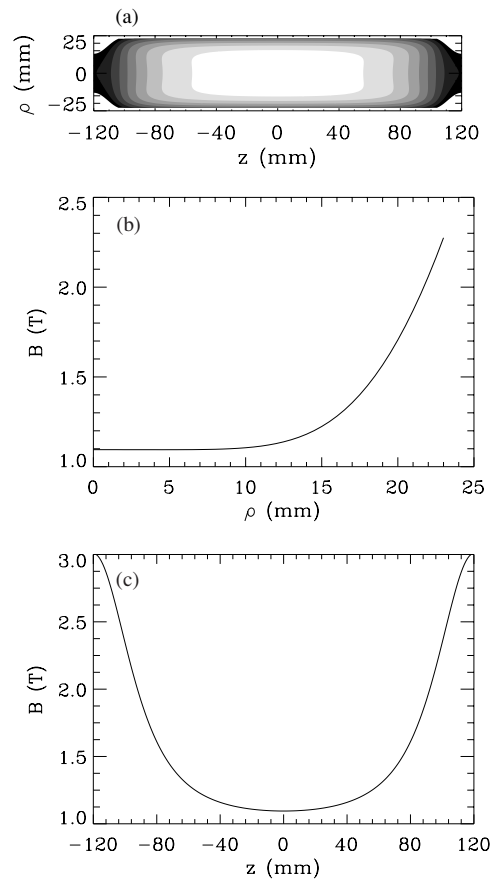
Figure 1. The magnitude of the magnetic field within the trap. (a) A contour plot showing the full spatial dependence of the field. The minimum of the field is near $(0, 0)$ with a value of approximately 1.1 T. The contours start at 1.25 T and increase in steps of 0.25 T. Note the large white region with B between 1.1 and 1.25 T. (b) A slice showing B versus distance from the centre of the trap to the wall. (c) A slice of the contour plot showing B versus position along the trap axis; the mirror coils are at ± 12 cm.

and a current of 11.5 kA; this high current results from our approximation of each mirror coil as a single wire loop. The field from the loop was calculated numerically using the Biot-Savart law with the circle approximated by 128 straight line segments and is approximately 2 T at the centre of a single coil. For the multipole field we used $s = 4$ and we had the strength of the this field be 2 T at the wall. To reach the trap wall $\bar{\text{H}}$ experience a change in magnetic field of at least 1.18 T which corresponds to 0.79 K trap depth for the ground state.

The total field is constructed from these simple elements. The largest error is from approximating the mirror coils as a single loop with the largest error being near the mirror coil *and* near the wall of the trap. However, the magnetic field is largest in this region. Therefore, we do not expect the trapped $\bar{\text{H}}$ to reach the region of least physical B. In figure 1, we show a contour plot of the magnitude of the magnetic field within the trap as well as two cuts of the magnetic field: one for $z = 0$ and the other for $\rho = 0$. It is clear that the magnetic field has a broad region where it changes little from its minimum value which is approximately 1.1 T. The high order of the multipole field causes the magnetic field to be relatively flat for a large

fraction of the distance to the wall with a very steep increase near the wall. For example, the magnetic field has increased by only 0.01 T in going from $\rho = 0$ to $\rho = 10$ mm at $z = 0$. The rise in B due to the mirror coils is less steep but occurs over much larger distance which gives a smaller increase over comparable distances. For example, the magnetic field has increased by 0.01 T in going from $z = 0$ to $z = 17$ mm at $\rho = 0$.

4. Types of cascade

The centre-of-mass energy of H̄ decreases with time because whenever a photon is emitted the magnetic moment can decrease. We distinguish between two cases. The adiabatic cascade is when the atom has time to oscillate in the trap between cascades. The sudden cascade is when the time between photon emissions is short enough that the atom hardly moves during the cascade. The purpose of this section is to give a physical interpretation of the results of our simulations.

4.1. Adiabatic cascade

For n that are not very large (larger than ~ 20), the radiative cascade is slow enough that the atom moves substantial distances between decays. Since the atom randomly emits a photon and several photons are emitted during a cascade, we examine the average energy lost by an atom if it is at a certain energy but emits at a random time in the orbit.

As an example, suppose the atom moves in a one-dimensional potential with the form $U(x) = Cx^{2\alpha}$. We can relate the time average of U and the kinetic energy to the energy, $E = \langle KE \rangle + \langle U \rangle$. Through the virial theorem $\langle x^{2\alpha} \rangle = E/[(\alpha + 1)C]$ if the time average is long enough. The average change in energy if C suddenly changes by an amount ΔC is

$$\frac{\Delta E}{E} = \frac{1}{\alpha + 1} \frac{\Delta C}{C}. \tag{7}$$

If the changes are small we can take the changes to be differentials and solve for E to find $(E/E_0)^{\alpha+1} = C/C_0$, where E_0 and C_0 are the starting values of C. This equation suggests that the per cent change in energy will be less than the per cent change in the coefficient C. For example, if $\alpha = 3$ and $C = (1/2)C_0$ then E only decreases by 16%: $E \simeq 0.84E_0$.

4.2. Sudden cascade

The radiative decay rate increases dramatically as n decreases. The type of cooling changes from adiabatic to a 'sudden' cascade over a small range of n. In the sudden cascade, the atom hardly moves while many photons are emitted: $n \rightarrow n - 1 \rightarrow \cdots 2 \rightarrow 1$. During this cascade the magnetic moment rapidly changes from several Bohr magnetons to $\pm 1\mu_B$. If the spin of e^+, gives an atom attracted to high fields, then the atom will be rapidly pulled to the walls to annihilate. If the spin gives an atom attracted to low fields, the atom will be trapped if its total energy is below the trapping well depth. Thus, whether an atom attracted to low fields remains trapped or not depends on the kinetic energy of the atom when it reaches n where the cascade can be considered sudden. Since the kinetic energy decreases as the atom moves to larger potential, there is a volume of space outside which if the atom begins its sudden cascade it will be trapped.

As an example, suppose the atom moves in a one-dimensional potential with the form $U(x) = C_0x^{2\alpha}$, where C_0 is a constant and α is an integer. If C_0 suddenly changes to $C_f \ll C_0$ when the atom is at position x_c, the atom loses energy equal to $(C_f - C_0)x_c^{2\alpha}$. If the atom is near a turning point where the kinetic energy is much less than the energy, then the atom

can lose most of its energy in this process. We can compute the fraction of atoms that end with energy less than E_f if we know the original energy of the atom, E_0, and the position dependence of the probability density, $P(x)$. All atoms that are at a position $|x| > x_f$ will have energy less then E_f when $x_f = [(E_0 - E_f)/(C_0 - C_f)]^{1/(2\alpha)}$. The fraction of atoms with final energy less than E_f is

$$f_t = \int_{x_f}^{x_{\max}} P(x)\,\mathrm{d}x + \int_{-x_{\max}}^{-x_f} P(x)\,\mathrm{d}x, \tag{8}$$

where $x_{\max}$ is the largest distance the atom can reach when the constant is C_0 and the energy is E_0: $x_{\max} = (E_0/C_0)^{1/(2\alpha)}$. We note that $x_f < x_{\max}$ when $C_f/C_0 < E_f/E_0$. This means that it is only possible to reach final energies E_f in proportion to the fractional change in C; for example, it is not possible to reach energies a factor of 10 less than the starting energy if C only changes by a factor of 5. Note that the higher the power of the potential, the more narrow is the region of space over which large energy can be lost. If the probability for the atom to be at x is proportional to the inverse of the velocity and it has energy E_0 with coefficient C_0, then the probability density is

$$P(x) = \left(\frac{C_0}{E_0}\right)^{\frac{1}{2\alpha}} \frac{\Gamma\left(\frac{\alpha+1}{2\alpha}\right)}{2\sqrt{\pi}\,\Gamma\left(\frac{2\alpha+1}{2\alpha}\right)} \frac{1}{\sqrt{1 - C_0 x^{2\alpha}/E_0}}. \tag{9}$$

If $x_f \sim x_{\max}$ then the integrals have a simple form which gives the fraction with final energy less than E_f:

$$f_t \simeq \frac{\Gamma\left(\frac{\alpha+1}{2\alpha}\right)}{\alpha\sqrt{\pi}\,\Gamma\left(\frac{2\alpha+1}{2\alpha}\right)} \sqrt{\frac{E_f}{E_0} - \frac{C_f}{C_0}} \tag{10}$$

which in the limit of large α becomes $f_t \simeq (1/\alpha)\sqrt{(E_f/E_0) - (C_f/C_0)}$. This shows that the fraction of trapped atoms becomes less as the power of the potential increases, but it is not a very fast decrease.

Another interesting way of looking at the problem is the probability density for the atom to have final energy E_f. Writing the final energy as a function of cascade position as $E_f = E_0 + (C_f - C_0)x^{2\alpha}$ and using the position-dependent probability density from equation (9) gives $\mathcal{P}(E_f) = (\mathrm{d}x/\mathrm{d}E_f)P(x)$:

$$\mathcal{P}(E_f) \propto \frac{1}{(E_0 - E_f)^{\frac{2\alpha-1}{2\alpha}}\left(E_f - \frac{E_0 C_f}{C_0}\right)^{1/2}}, \tag{11}$$

where $E_0 C_f/C_0$ is the lowest possible final energy. Note this gives integrable singularities at the lowest and highest possible final energies with a single minimum between those limits.

5. Results

In this section, we describe the results of various calculations that demonstrate how $\bar{\mathrm{H}}$ can cool during the radiative cascade. The calculations allow for realistic estimates of the size of this effect for a reasonable $\bar{\mathrm{H}}$ trap. The calculations also show that the hit pattern on the wall of the trap is substantially broadened when Rydberg $\bar{\mathrm{H}}$ exist in the trap.

5.1. Cooling

In this section, we will discuss the centre-of-mass cooling of $\bar{\mathrm{H}}$ due to the radiative cascade. In the last step of the cascade, the atom reaches the 1s state and all of the trapping is due to
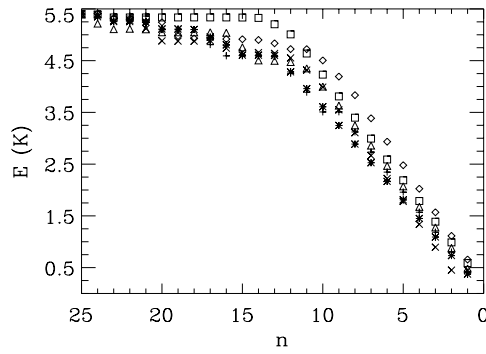
Figure 2. The centre-of-mass energy of H̄ as a function of the principal quantum number for several atoms that are trapped at the end of the cascade. All atoms start with 5.4 K of energy in the $n = 25$ circular, state: $m \simeq n$. The atoms move perpendicular to the trap axis which is the least favourable geometry for cooling. There is little cooling from $n = 25$ to ~ 13 because the time between photon emissions is large: the atom emits photons in regions of high and low B. Most of the cooling occurs for n less than ~ 13 because the cascade is rapid: the atoms hardly move so those at high B lose most of their energy.

the magnetic moment from the spin of e^+. Presumably, one half of the atoms will finish as atoms attracted to high fields and half will be attracted to low fields. However, there could be a substantial difference from this population due to the starting spin of the electron, preferences in the radiative cascade, or other processes. Since we do not know what will be the fraction of atoms attracted to high versus low fields for the ground state, *we give all our results in this section assuming 100% population is attracted to low fields.* When the population becomes known, the results of this section can be multiplied by the appropriate factor.

In figure 2, we give the total energy of an atom as a function of principal quantum number when the atom starts in a circular state. The principal quantum number started at $n = 25$. The atom started at the origin with 5.4 K of kinetic energy ($v \simeq 300$ m s^{-1}) with the motion directed perpendicular to the trap axis. Figure 2 only shows examples of atoms that finish with energy less than 0.79 K. Note that they have similar dependence of E on n. For the n range 25 to ~ 13, there is relatively little energy that is lost on average, roughly ~ 0.7 K. The major portion of the energy is lost as the atom cascades from ~ 13 to 1. This graph is showing the difference in energy loss due to the adiabatic cascade and the sudden cascade. Because we are starting in circular states, there is approximately the same change in magnetic moment when going from $n = 25$ to 13 as when going from 13 to 1. Using the analysis from section 4.1 we would expect the energy to decrease by a factor of ~ 0.84 since $\alpha = 3$ and $C_f/C_0 \simeq 1/2$. This would give a decrease of 0.16×5.4 K which is 0.86 K, slightly more than in our simulation. The large energy change during the sudden part of the cascade is from the fraction of atoms that are near their turning point. From equation (10), we would expect approximately 8% (using $E_f/E_0 = 0.79/4.7$ and $C_f/C_0 = 1/13$ with $\alpha = 3$) to finish with energy less than 0.79 K whereas our simulation gave 11%. Both the estimate of energy lost during the adiabatic cascade and the estimate of the fraction of atoms that finish with energy less 0.79 K are in good agreement with the simulations.

One can qualitatively understand that the adiabatic cascade gives less cooling because the photon can be emitted in regions where B is small as well as high, but the sudden cascade only focuses on the atoms that emit a large number of photons where B is large. Because the adiabatic cooling is not very effective at removing energy, increasing the principal quantum number does not give a significant increase in the cooling.
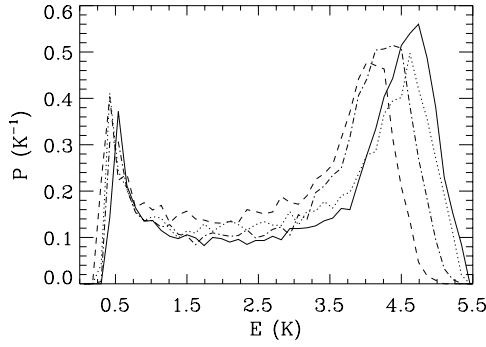
Figure 3. The energy distribution of atoms after they have reached $n = 1$. The atoms start with $n = 25$ and 5.4 K of energy ($v \simeq 300$ m s^{-1}) from the exact centre of the trap. The solid and dot-dashed lines are for atoms that travel from the centre of the trap, perpendicular to the axis. The dotted and the dashed lines are for atoms that travel along the trap axis. For the dot-dashed and the dashed lines, the atoms start in circular $m \simeq n$ states. For the solid and dotted lines, the atoms start in a random distribution of $m \geqslant 15$ as described in the text. The shape of the distributions can be understood from the properties of a sudden cascade.

In figure 3, we show the distribution of final energy for atoms that start at the origin with principal quantum number $n = 25$ and 5.4 K of kinetic energy. There are four curves: two for atoms with velocity purely along the axis and two for atoms with velocity perpendicular to the axis. For each type of motion, we show the cascade for atoms that start in circular states $m \simeq n$ and for atoms that start in a random distribution of m from 15 to 24 with ℓ randomly distributed for each m. There are several features that stand out. The first is that all curves have a two-peaked structure with the peaks at the end of the range. This is the energy distribution expected from the sudden cascade equation (11). Note that the position of the upper peak is reduced from 5.4 K. This is due to the adiabatic cooling that occurs during the cascade from $n = 25$ to ~ 13. Another feature is that each distribution from atoms that start in circular states has more atoms at lower energy *and* the upper energy peak is lower in energy by 0.4–0.5 K compared to the corresponding distribution of atoms with an initial spread in m. Finally, the distribution for atoms moving along the axis has more atoms at lower energy and the peaks are shifted to lower energy than for the atoms moving across the axis. This is because the potential across the axis is flatter over a larger fraction of the range; this means there is a smaller fraction of the region where the atom can emit a photon while at high B.

For figure 3, we ran 10 000 trajectories for each curve. For each run we computed the fraction of atoms that ended with energy less than 0.79 K which corresponds to being trapped for the magnetic fields we used. For the atoms starting in circular states ($m \simeq n$), 14% of the atoms were trapped when travelling along the axis while 11% were trapped when travelling perpendicular to the axis. For the atoms starting with a range of m, 12% were trapped when travelling along the axis while 10% were trapped when travelling perpendicular to the axis. Therefore, it seems that this effect will be present so long as there is a population of atoms with large m. Note that *none* of these atoms would be trapped without cooling.

To this point, we have examined what happens if the atoms start at a specific point and is moving along a symmetry direction. In the $\bar{\text{H}}$ experiments, $\bar{\text{H}}$ will be formed, approximately uniformly, in the region of the e$^+$ plasma. In the best case, the $\bar{\text{H}}$ will form with energy comparable to that of the e$^+$ plasma. In figure 4, we give the final energy distribution when we start the atoms with a thermal velocity distribution corresponding to 4 K and initial principal quantum number of $n = 25$. The atoms are started randomly within a spheroidal region
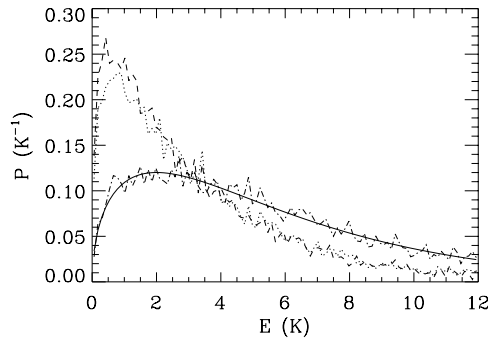
Figure 4. Same as figure 3 except the atoms start in a thermal distribution with a temperature of 4 K and have an initial spatial spread described in the text. The dashed line is for atoms starting in a circular state while the dotted line is for atoms in a random distribution of $m \geqslant 15$. The dot-dashed line shows the initial distribution and the solid line is the thermal distribution: $\propto \sqrt{E} \exp(-E/k_B T)$. As in figure 3, substantial cooling occurs with the circular states showing a slightly stronger effect.

$(x^2 + y^2)/\rho_e^2 + z^2/z_e^2 < 1$, where ρ_e and z_e are constants that determine the width and length of the e$^+$ plasma. We took $\rho_e = 2$ mm and $z_e = 15$ mm. We show two cases, one of which corresponds to the $m \simeq n$ distribution and one of which corresponds to the random m between 15 and 24. The distribution of initial energies is shown with the analytic thermal distribution overlaid. The distributions have a quite different appearance from those in figure 3 due to the broad range of starting energies. However, it is clear that the energy distribution after the cascade has more atoms at lower energy. For the atoms starting in the circular state, 18% were trapped compared to 16% for random m; only 6% of the initial distribution would be trapped.

For this size plasma, we computed the average time an $n = 25$ atom spent within the plasma before a photon was emitted. For the circular states, the atom spent ∼20 μs inside the plasma whereas the atom spent ∼15 μs inside the plasma for random m between 15 and 24. This indicates that plasmas of this shape with densities of 10^7 cm^{-3} will not give a significant amount of scattering, but densities ten times higher could cause problems.

5.2. Hit pattern

The temporary trapping of Rydberg H̄ also leads to a change in the distribution of annihilations on the walls of the trap. This arises because H̄ form in a small region. If the atoms are temporarily trapped, they will bounce around inside of the trap until the magnetic moment decreases too far and the atom reaches the walls. However, this process occurs at a random time which means the position distribution of the annihilations will be broader in z compared to the situation without trapping.

In figure 5, we show four distributions of annihilations when H̄ are formed in the same size region as for figure 4. In all of the calculations, the atoms start with a thermal velocity distribution with a temperature of 4 K with principal quantum number $n = 25$. The solid line is if there is no spatial dependence to the magnetic field or, equivalently, the magnetic moment is set to zero. In this case, the atoms move in straight lines until they hit the wall and the distribution is simply a geometrical effect. The dot-dashed line is when all of the atoms are strongly attracted to high fields: $m \simeq -n$. As soon as the atoms move from the region of flat potential, they are pulled to high magnetic fields. Finally, the dashed line is when all of the atoms are strongly attracted to low fields ($m \simeq n$) and the dotted line is when m is random but
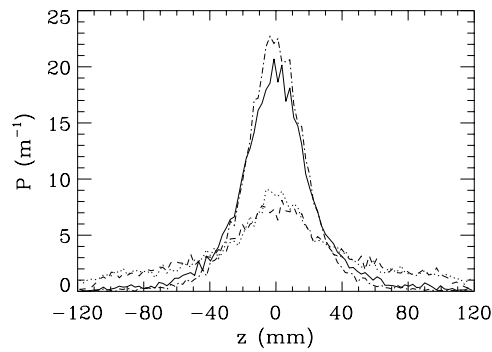
Figure 5. The distribution of annihilations on the wall of the trap as a function of z. The atoms have the same initial properties as in figure 4. The dotted and the dashed lines are for the same distribution as figure 4. The solid line shows the distribution of hits if there were no trapping fields on. The dot-dashed curve shows the distribution of hits for atoms attracted to high fields.

much greater than 1. Many of the trends in the distributions can be understood from general arguments. The atoms attracted to high fields have the most hits near the region where $\bar{\text{H}}$ is formed because they are attracted to the walls, but the change from no magnetic moment is not large. This is because of the high multipole moment of the B-field which pulls the atom to the wall; the atoms travel in straight lines for a large distance before entering the region where the force from the B-field can begin deflecting its path. However, the most interesting feature is that the atoms attracted to low fields have a very broad distribution in z. Note that the ratio of the number of hits near $z = 0$ to that near 75 mm is roughly 1/5 for the atoms attracted to low fields but is approximately 1/50 for atoms with zero magnetic moment and even less for the atoms attracted to high fields.

This suggests a diagnostic for the $\bar{\text{H}}$ experiments. The distribution of annihilations along the trap can serve as an indicator of trapped, Rydberg $\bar{\text{H}}$. The distribution should not extend far from the formation region ($z \sim 0$) if the multipole trapping field is turned off. But if that field is on, then the distribution should decrease near $z = 0$ and increase far away from that region.

6. Conclusions

We have shown that the spatially varying magnetic field in the next generation $\bar{\text{H}}$ experiments will not only act to trap the atoms but will also lead to cooling of the centre-of-mass motion for atoms that initially form in Rydberg states with large magnetic moment. The fraction of cooled atoms depends on the properties of the initial state and the spatial dependence of the magnetic field. However, the size of the effect can be substantial.

If atoms are formed with large positive magnetic moments, the cascade can lead to cooling and trapping. However, most of the atoms will not be trapped unless the temperature of $\bar{\text{p}}$ is much less than that expected in the next generation of $\bar{\text{H}}$ experiments. Many of $\bar{\text{H}}$ will start with a large enough magnetic moment to be initially trapped by the magnetic fields but during the radiative cascade they will reach a stage where the magnetic moment has decreased to the point where the trap depth is insufficient. $\bar{\text{H}}$ will then be able to reach the wall and annihilate. Because $\bar{\text{H}}$ will have travelled a substantial distance during the cascade, it is much more likely to hit the wall of the trap far from where it is made. Thus, a signature of a population of trapped Rydberg $\bar{\text{H}}$ will be the distribution of hits on the walls of the trap.

Acknowledgments

References

[1] Amoretti M *et al* (ATHENA Collaboration) 2002 *Nature* **419** 456
[2] Gabrielse G *et al* (ATRAP Collaboration) 2002 *Phys. Rev. Lett.* **89** 213401
[3] Gabrielse G *et al* 1988 *Phys. Lett.* A **129** 38
[4] Glinsky M E and O'Neil T M 1991 *Phys. Fluids* B **3** 1279
[5] Robicheaux F and Hanson J D 2004 *Phys. Rev.* A **69** 010701
[6] Hessels E A, Homan D M and Cavagnero M J 1998 *Phys. Rev.* A **57** 1668
[7] Storry C H *et al* 2004 *Phys. Rev. Lett.* **93** 263401
[8] Wall M L, Norton C S and Robicheaux F 2005 *Phys. Rev.* A **72** 052702
[9] Robicheaux F 2004 *Phys. Rev.* A **70** 022510
[10] Gabrielse G *et al* (ATRAP Collaboration) 2004 *Phys. Rev. Lett.* **93** 073401
[11] Madsen N *et al* (ATHENA Collaboration) 2005 *Phys. Rev. Lett.* **94** 033403
[12] Robicheaux F 2006 *Phys. Rev.* A **73** 033401
[13] Hessels E A private communication
[14] Pohl T, Sadeghpour H R, Nagata Y and Yamazaki Y private communication
[15] Topçu T and Robicheaux F 2005 *Phys. Rev.* A **73** 043405
[16] Fajans J, Bertsche W, Burke K, Chapman S F and van der Werf D P 2005 *Phys. Rev. Lett.* **95** 155001
[17] Jackson J D 1999 *Classical Electrodynamics* (New York: Wiley) p 770